



Published in final edited form as:

J Biomater Appl. 2014 October ; 29(4): 514–523. doi:10.1177/0885328214535452.

Chitosan coating to enhance the therapeutic efficacy of calcium sulfate-based antibiotic therapy in the treatment of chronic osteomyelitis

Karen E Beenken¹, James K Smith², Robert A Skinner³, Sandra G McLaren³, William Bellamy⁴, M Johannes Gruenwald³, Horace J Spencer⁵, Jessica A Jennings², Warren O Haggard², and Mark S Smeltzer^{1,3}

¹Department of Microbiology and Immunology, University of Arkansas for Medical Sciences, Little Rock, AR, USA

²Department of Biomedical Engineering, University of Memphis, Memphis, TN, USA

³Department of Orthopaedic Surgery, University of Arkansas for Medical Sciences, Little Rock, AR, USA

⁴Department of Pathology, University of Arkansas for Medical Sciences, Little Rock, AR, USA

⁵Department of Biostatistics, University of Arkansas for Medical Sciences, Little Rock, AR, USA

Abstract

We demonstrate that coating calcium sulfate with deacetylated chitosan enhances the elution profile of daptomycin by prolonging the period during which high concentrations of antibiotic are released. Coatings reduced initial bolus release of daptomycin by a factor of 10 to approximately 1000 µg/ml, and levels remained above 100 µg/ml for up to 10 days. Chitosan-coated and uncoated calcium sulfate implants with and without 15% daptomycin were evaluated in an experimental model of staphylococcal osteomyelitis through bacteriology scores, radiology, histopathology, and Gram staining. Significant reduction in bacteriology scores was observed for implants containing daptomycin and coated with chitosan compared with all the other groups. We confirm that the use of chitosan-coated calcium sulfate beads for local antibiotic delivery can be correlated with an improved therapeutic outcome following surgical debridement in the treatment of chronic osteomyelitis.

Keywords

Calcium sulfate; daptomycin; local drug delivery; osteomyelitis; chitosan; bone; infection

© The Author(s) 2014

Corresponding author: Jessica A Jennings, 330 Engineering Technology Building, Memphis, TN 38152, USA., jjennings@memphis.edu.

Conflict of interest

The content is the responsibility of the authors and does not necessarily represent the views of the NIH or Department of Defense.

Introduction

Infections of bone and indwelling orthopaedic devices are recalcitrant to conventional antibiotic therapy, irrespective of the acquired resistance status of the offending bacterial strain.¹ There are several reasons for this, but one primary contributing factor is the formation of a bacterial biofilm, the presence of which confers a therapeutically relevant degree of intrinsic resistance to both host defenses and conventional antibiotics.^{2,3} For this reason, treatment of these infections most often involves surgical debridement accompanied by some form of localized antibiotic delivery, the goal of the latter being to achieve a high-enough concentration of antibiotic at the site of infection to overcome this intrinsic resistance while avoiding systemic toxicity.^{1,4}

The manner in which localized antibiotic delivery is accomplished depends on the extent of debridement required.⁵ In those cases in which debridement creates a structurally unstable defect that will ultimately require stabilization using orthopaedic hardware, the most common delivery vehicle is polymethylmethacrylate (PMMA) bone cement beads, primarily because PMMA is not biodegradable and therefore does not alter the wound site prior to reconstruction.⁶ However, for the same reason, antibiotic-loaded, PMMA beads must be removed before reconstruction. Additionally, PMMA has a poor elution profile, characterized by an initial bolus release of relatively high concentrations followed by a rapid decline to sub-inhibitory concentrations. Overall, antibiotic recovery from the beads is also poor, thus adding considerable cost without therapeutic benefit. Thus, a primary goal in efforts to improve PMMA as a delivery vehicle is to increase porosity to an extent that prolongs the period during which antibiotic levels remain significantly above the breakpoint minimum inhibitory concentration (MIC) for any given antibiotic. We demonstrated that this is possible by incorporating xylitol, an inexpensive and biologically inert disaccharide with limited anti-biofilm properties in and of itself, into PMMA along with the appropriate antibiotics.⁷

Alternatively, in cases in which the debridement required is not so extensive that it creates a structurally unstable defect, it is preferable to use a biodegradable delivery matrix, thereby avoiding the need for a second procedure to remove the matrix prior to reconstruction.⁶ A common alternative in such cases is calcium sulfate (CaSO_4) α -hemihydrate, a biodegradable and biocompatible ceramic, that can also be loaded with water-soluble antibiotics.⁸⁻¹⁰ Dissolution of CaSO_4 also provides an osteoconductive environment that enhances vascular ingrowth and osteogenesis. Overall, antibiotic recovery is also higher by comparison to PMMA. However, the elution profile is still characterized by an initial burst that quickly diminishes as the CaSO_4 dissolves.^{11,12} In fact, the decline is generally even more rapid than that observed with PMMA. Thus, the goal in this case is also to prolong elution, however the approach to doing so is different in that it is necessary to slow dissolution and thereby limit, rather than, enhance antibiotic elution. Slowing dissolution would also limit the osmotic effect in the localized wound environment that can lead to the formation of a seroma that requires surgical drainage.¹³

To accomplish this task, we explored the use of chitosan as a coating for antibiotic-loaded CaSO_4 beads. Chitosan is a biocompatible polymer that degrades into simple sugars by

enzymatic hydrolysis. It is produced commercially by deacetylation of chitin (Figure 1), the structural element of the exoskeleton of crustaceans, and it is available commercially in a highly purified form for biomedical applications.¹⁴ It is also currently used as an FDA-approved hemostatic agent (HemCon Medical Technologies, Portland, OR) to control hemorrhaging of battlefield injuries.^{15,16} Chitosan is also highly “tunable” in that the degree of deacetylation can be adjusted to achieve the desired elution and degradation characteristics, and it can be produced in alternative forms that include films appropriate for coating orthopaedic implants as a means of preventing infection.^{17,18} Chitosan itself has antibacterial properties^{19,20} and promotes wound healing.²¹ Indeed, a chitosan sponge developed by our group recently received FDA clearance for marketing as a wound dressing (see 510(K) at the FDA website (<http://www.accessdata.fda.gov/scripts/cdrh/devicesatfda/index.cfm?db=pmn&id=K112191>)).

Thus, chitosan offers many advantages as a coating for CaSO₄ and as a stand-alone antibiotic delivery vehicle. Chitosan has not yet been approved by the FDA for this specific purpose, but we and others^{17,22,23} have begun to explore these advantages. In this manuscript, we report the results of some of these studies carried out in the specific context of using chitosan-coated CaSO₄ pellets containing daptomycin in the post-debridement treatment of chronic osteomyelitis.

Materials and methods

CaSO₄ formulation and characterization

The CaSO₄ α-hemihydrate (Osteoset[®], Wright Medical Technology, Arlington, TN) pellet formulations evaluated in these experiments included CaSO₄ alone, CaSO₄ coated with chitosan (Cognis, Chitopharm[®]; Monheim, Germany; degree of deacetylation: 78%, average molecular weight: 2.1×10² kDa), CaSO₄ loaded with daptomycin (Cubicin[®]; Cubist Pharmaceuticals, Lexington, MA), and CaSO₄ with both daptomycin and a chitosan coating. We chose to focus on daptomycin because we have previous experience with this antibiotic in our studies focusing on PMMA and because it exhibits greater therapeutic efficacy than many other antibiotics in the context of a biofilm.³

Pellets without antibiotic were created by mixing 12 g CaSO₄ in 3.71 ml of 0.172M K₂SO₄. The resulting putty was cast into a custom made, 4mm×10 mm, cylindrical, silicone template (Sylgard 170 Silicone Elastomer, Dow Corning; Midland, MI), which approximates the size of an excised rabbit radial segment (Figure 1), and allowed to cure for 15 min. For antibiotic loading, 8.5 g of CaSO₄ putty was added to 3.09 ml of K₂SO₄ and mixed for 1 min before adding 1.5 g of daptomycin powder (Cubicin[®], Cubist Pharmaceuticals, Lexington, MA) and placing the slurry into the mold. Thus, the weight to volume ratio in both cases was ~3.2, with daptomycin representing 15% of the total weight in daptomycin-loaded pellets. The daptomycin-loaded CaSO₄ was allowed to cure for 45 min, the increased time being necessary due to the presence of antibiotic. Although calcium is required for the activity of daptomycin, no calcium was added to either pellet formulation because it is available in vivo.

For chitosan coatings, CaSO₄ pellets were submerged in a viscous solution of 4 w/v% chitosan in 0.26M lactic acid. The pellet was then allowed to completely dry in a desiccator at room temperature. The coating procedure was repeated five times to provide uniform coverage of the chitosan, with the average coating thickness ranging from 0.4 to 0.8 mm. All pellets were stored at room temperature in a desiccator until elution testing or evaluation in our rabbit osteomyelitis model.

To determine the effect of chitosan coating on the elution of daptomycin, in vitro elution comparisons were performed by dividing daptomycin-loaded pellets into sample sets consisting of four pellets each, with each set of four being repeated in triplicate. Each set was placed in a flask containing 6 ml of sterile phosphate-buffered saline (PBS) and incubated at 37°C with constant shaking for 10 days. At 24-h intervals, the entire volume of PBS was removed and replaced with 6 ml of fresh, sterile PBS, thus ensuring that antibiotic obtained on any given sampling day was eluted since the previous sampling day. Samples were stored at -20°C until analysis using high-pressure liquid chromatography with a C₈ column and an acidic acetonitrile-salt mobile phase.^{7,24} Quantitative measurements were made by comparison to a standard curve generated using suspensions with a known concentration of daptomycin ranging from above the maximum and below the minimum observed in our experimental samples. The calibration curve correlated the peak area to the known concentration. Peak area regression analysis was performed on calibration standards to obtain a best fit line. Unknown sample peak areas were then converted to concentration using the regression equation.

Rabbit osteomyelitis model

All in vivo experiments were done in accordance with the policies of the Public Health Service on the care and use of laboratory animals, the Animal Welfare Act, and the NIH Guide for the Care and Use of Laboratory Animals. All animal procedures were reviewed and approved by the Institutional Animal Care and Use Committee of the University of Arkansas for Medical Sciences and carried out in an Association for Assessment and Accreditation of Laboratory Animal Care accredited facility.

Therapeutic efficacy was assessed using an established rabbit model of postsurgical osteomyelitis.^{7,25} Briefly, a 1-cm midradial segment was surgically excised from each of 24 male, New Zealand white rabbits. For the preparation of inocula, methicillin-sensitive *Staphylococcus aureus* osteomyelitis isolate UAMS-1 was grown overnight in tryptic soy broth at 37°C with constant aeration. The cultures were harvested by centrifugation, washed with equal volumes of sterile physiological saline, and resuspended in sterile saline to an optical density of 1.0. Each standardized suspension was plated on tryptic soy agar (TSA) to ensure a cell density of approximately 2×10^8 colony-forming units per ml. Standardized suspensions were kept on ice throughout the surgical procedure. Additionally, plate counts were repeated after the surgery to ensure the purity and density of each cell suspension. The standard inoculum (2×10^6 colony-forming units) was delivered by microinjection of 10 μ l of the standardized suspension directly into the medullary canal of the excised bone segment. UAMS-1 was also confirmed to be sensitive to daptomycin at concentrations below the MIC of 1.0 μ g/ml by E-test as previously described.³ The segment was then returned to the radial

defect in its original orientation, and the wound was closed. After 3 weeks, radiographs were obtained from all rabbits prior to opening the incision site and performing a minimal debridement limited to removal of the 1-cm infected bone segment and irrigation with 50 ml of sterile PBS. This debridement was minimized to ensure that the infection was not cleared by debridement alone. Samples for bacteriological analysis were taken from the bone and surrounding soft tissue before and after debridement. After debridement, the defect was filled with a single pellet manufactured to fit snugly into the 1-cm defect (Figure 1) from one of the following four groups: CaSO₄ without antibiotics and without chitosan coating (0 U), CaSO₄ without antibiotics with chitosan coating (0 C), 15% daptomycin-loaded CaSO₄ without chitosan coating (15 U), or 15% daptomycin-loaded CaSO₄ with chitosan coating (15 C). Rabbits were randomized by treatment group (n=6), with only one technician in the operating suite aware of the CaSO₄ formulation placed into each rabbit following debridement.

Assessment of relative therapeutic efficacy

Pellets were left in place for 3 weeks without any additional form of antibiotic treatment, at which time rabbits were humanely euthanized, and the surgical limb was harvested for X-ray, histological, and bacteriological analysis as previously described.⁷ For bacteriological analysis, samples were collected by swab from the infection site and used to inoculate TSA without antibiotic selection. To achieve a quantitative comparison, swabs were used to comprehensively inoculate the first quadrant of a TSA plate, which was then struck for isolated colonies using standard bacteriological techniques. The relative amount of growth was scored after 24 h at 37°C based on growth in the first quadrant only (1+) to growth across all four quadrants (4+). The scores obtained with all swabs from each experimental animal were then averaged to obtain a single bacteriological score. The same scoring protocol was employed immediately before and after debridement, thus yielding three bacteriological scores for each rabbit. However, because the critical issue was the relative therapeutic response, the primary analysis was based on scores for each rabbit obtained after debridement and after treatment. As a control for variation between rabbits, these scores were used to calculate the average change in bacteriological score between these time points.

X-rays were scored by an orthopaedic surgeon blinded to the infection status of each rabbit. Scores were based on evidence of periosteal elevation, sequestration, architectural deformation, and deformation of soft tissue as previously described.⁷ Each parameter was scored on a 5-point scale (0 to 4), with 4 representing the most severe evidence of disease. Scores were then averaged to obtain a single radiographic score for each rabbit at both the debridement and post-treatment time points. As with our bacteriological analysis, we then calculated the average change in overall radiographic scores within each experimental group.

After collection of the final samples for bacteriological analysis, the surgical limb was removed and processed for histological analysis by hematoxylin and eosin staining and by Gram stain.²⁵ However, the histopathological scoring system was modified as previously described to address the inclusion of a treatment phase in these experiments.⁷ A separate

score was also derived for each rabbit based on Gram stain and the relative abundance of intraosseous Gram-positive cocci. Given the osteoconductive properties of CaSO₄, we also assessed new bone growth as a separate experimental parameter, but only in the post-treatment group, because this was the only time point at which all animals had been exposed to CaSO₄.⁷

Statistical analysis

We determined the effect of chitosan coating on daptomycin elution between the different groups using two-way ANOVA with Tukey's post hoc analysis. Similarly, two-way ANOVA was used to determine whether various CaSO₄ formulations differed with respect to bacteriology, X-ray, histology, and Gram stain scores. If significant, Tukey's post hoc tests were used to perform pairwise testing. Statistical significance for all analyses was determined using an α level of 5%.

Results

Our in vitro elution studies demonstrate two important changes in the CaSO₄ elution profile of daptomycin that were attributable to coating with chitosan. First, the initial bolus release was reduced approximately 10-fold (Figure 2). However, the maximum concentration observed after 1 day of elution even with chitosan coating was ~1000 µg/ml or ~1000 times (1000×) the breakpoint MIC for daptomycin. Second, without chitosan coating, the concentration of antibiotic eluted from the pellets fell rapidly, going below an arbitrarily chosen standard of 100 times (100×) the breakpoint MIC for daptomycin by day 3. In contrast, with chitosan-coated CaSO₄ pellets, the concentration of daptomycin remained well above this standard even after 10 days (Figure 2). In fact, during the period between 6 and 10 days, the amount of daptomycin obtained with chitosan-coated pellets was >50-fold higher than that obtained with uncoated pellets. Taken together, these results confirm that coating with chitosan is an effective method to extend antibiotic elution from CaSO₄ without an unacceptable compromise of the maximum levels obtainable during the early stages of elution.

Bacteriological analysis confirmed that the infection status in all experimental groups was roughly equivalent both before (data not shown) and immediately after debridement (Figure 3). It also demonstrated that overall bacteriological scores were significantly lower in the group treated with chitosan-coated pellets containing daptomycin (15 C) than in the untreated (CaSO₄ alone) control group (0 U). There was no statistically significant difference between the untreated control group (0 U) and the group treated with uncoated, daptomycin-loaded pellets (15 U), which further suggests that coating with chitosan did have a positive therapeutic effect. However, when the results were evaluated based on the change in bacteriological scores between the time of debridement and after treatment, there was no significant difference between the daptomycin-treated groups depending on whether CaSO₄ pellets were coated with chitosan (Figure 3).

These same overall trends were also observed when the analysis was based on overall radiographic scores, although in this case, none of the differences between experimental groups were statistically significant (Figure 4). No such trends were noted based on overall

histopathological scores or Gram stain analysis (Figures 5 and 6). In fact, the opposite appeared to be true, with overall histopathological scores being highest in the experimental group treated with chitosan-coated CaSO₄. New bone growth was also comparable in all groups (Figure 7).

Discussion

The in vitro elution profile we targeted in our earlier studies focusing on PMMA (a maximum concentration at least 100 times (100×), the breakpoint MIC of 1.0 µg/ml and a sustained concentration defined after 10 days of continuous elution of at least 5× the breakpoint MIC) was chosen arbitrarily based on the recognized need to significantly exceed MIC of the offending bacterial strain in the specific context of a biofilm. However, when we transitioned to in vivo studies, it was also found to be inadequate based on a lack of any significant therapeutic response.⁷ For that reason, we increased the amount of daptomycin to 4 g per 40 g packet of PMMA. This resulted in an elution profile with a maximum concentration just over 1000 µg/ml and a sustained concentration just under 100 µg/ml, and with this formulation, we did observe an enhanced therapeutic effect.⁷ Based on this, we attempted to achieve a similar elution profile in the experiments reported here, a goal that we were able to accomplish only by coating CaSO₄ pellets with chitosan. By providing a physical barrier to slow the release of antibiotic, initial burst of daptomycin release from CaSO₄ was reduced, and active antibiotic concentrations were released for an extended period compared to studies using uncoated CaSO₄.^{10,26,27} A study by Zhang and Zhang²⁸ demonstrated that the calcium-containing component of a beta-tricalcium phosphate/chitosan composite improved release kinetics of gentamicin over chitosan alone. While chitosan coatings impede the release of the antibiotic daptomycin from a calcium-based carrier, they may increase release of some molecules such as protein growth factors like bone morphogenetic protein-2 (BMP-2) from calcium phosphate and CaSO₄ cements.^{29–32} A study by Doty et al.³³ demonstrated that embedding chitosan microbeads containing BMP-2 within a matrix of CaSO₄ served to slow growth factor release while maintaining active levels of released vancomycin over a period of 18 days in vitro. Composite formulations of hydroxyapatite, CaSO₄, and chitosan have improved the release profiles of vancomycin, fosfomycin, and amphotericin B over PMMA.^{34,35} The versatility of chitosan and its ability to be formed as coatings, films, microbeads, sponges, or as a material additive makes it valuable in controlling drug release for locally implanted biomaterials.^{18,23,36–38}

The more critical issue is whether this enhanced elution profile can be correlated with an improved therapeutic outcome, and we believe that the results we report support the conclusion that this is also true. This is based primarily on bacteriological analysis, which confirmed a statistically significant difference in the reduction in bacterial load in rabbits treated with chitosan-coated CaSO₄ pellets containing daptomycin (15 C) versus rabbits treated with CaSO₄ alone (0 U). Importantly, this was not true of any other experimental group including rabbits treated with uncoated pellets containing daptomycin (15 U). Improved availability of locally delivered daptomycin improved outcome compared to systemic and PMMA-delivered daptomycin in similar osteomyelitic models.^{39–41} We consider this a particularly significant observation given our purposeful use of a minimal debridement protocol.

The results were much less clear when the analysis was based on radiographic or histopathological evidence of disease or, for that matter, the presence of intraosseous Gram-positive cocci. This was also true in our experiments focusing on the use of xylitol as a means of enhancing antibiotic elution from PMMA,⁷ and as noted in that report, this is perhaps not surprising given that we used a high-bacterial inoculum to purposefully establish a severe infection in all rabbits and limited our debridement to a degree meant to ensure that this infection status was maintained at the outset of the treatment period. These evaluations add to the understanding of the effect of local antibiotic delivery systems on the progression or elimination of osteomyelitic disease state over studies using bacteriological methods alone.^{42–45} Practicality also imposes a time frame on studies like those we report, and it remains unclear whether a longer course of therapy or whether combining our protocol with systemic therapy would have further enhanced the therapeutic outcome as assessed based on these parameters. Similarly, there was little difference in overall Gram stain scores, but as was also noted in our previous report,⁷ these scores were based on the relative abundance of intraosseous Gram-positive cocci, and this does not mean that the bacteria present were viable. In fact, this seems unlikely given the definitive changes observed based on bacteriological scores, which were in fact based on the relative abundance of viable bacteria recovered from each rabbit.

Finally, new bone growth was also comparable between all experimental groups, but the significance of this, if any, must be interpreted with caution for several reasons. First, we did not include an experimental group without CaSO₄, and so the extent to which CaSO₄ alone promotes new bone growth in this osteomyelitic model remains unclear. Previous reports indicate that CaSO₄ antibiotic delivery vehicles support increased bone growth as they serve as an osteoconductive substrate while eliminating infectious complications.^{46–50} However, perhaps, the more important point is that, if any of the new bone growth observed is attributable to CaSO₄, it was not compromised by the presence of a chitosan coating, thus suggesting that the improved bacteriological outcome would not compromise other potential benefits of CaSO₄ in the context of localized antibiotic therapy in the treatment of chronic osteomyelitis. This is in agreement with the studies demonstrating the compatibility of chitosan and chitosan–CaSO₄ composites in the context of bone healing.^{36,51–57} Composites of chitosan and calcium phosphate, hydroxyapatite, and other biomaterials have been demonstrated to have positive effects on cell attachment, proliferation, and bone ingrowth.^{58–62} Antimicrobial properties of chitosan have been reported for several forms of chitosan in various uses, including implants and medicaments.^{63–68} In fact, while none of the differences in Gram-stain scores reached statistical significance, the scores were lowest in the two groups treated with chitosan-coated pellets irrespective of the presence of daptomycin, a result that suggests that chitosan itself may offer independent therapeutic benefits.

Acknowledgments

Funding

Research in the Smeltzer laboratory is supported by grants from the National Institute of Allergy and Infectious Disease (R01-AI069087, R56-AI074935, R56-AI093126); and the Department of Defense U.S. Army Medical Research and Materiel Command (W81XWH-10-1-0991, W81XWH-12-2-0020). Support was also provided by the

Translational Research Institute (UL1TR00039) through the NIH National Center for Research Resources and National Center for Advancing Translational Sciences and by the core facilities supported by the Center for Microbial Pathogenesis and Host Inflammatory Responses (P20-GM103450).

References

1. Cierny G III. Surgical treatment of osteomyelitis. *Plast Reconstr Surg.* 2011; 127(Suppl 1):190S–204S. [PubMed: 21200291]
2. Brady RA, Leid JG, Calhoun JH, et al. Osteomyelitis and the role of biofilms in chronic infection. *FEMS Immunol Med Microbiol.* 2008; 52:13–22. [PubMed: 18081847]
3. Weiss EC, Zielinska A, Beenken KE, et al. Impact of sarA on daptomycin susceptibility of *Staphylococcus aureus* biofilms in vivo. *Antimicrob Agent Chemother.* 2009; 53:4096–4102.
4. Rao N, Cannella B, Crossett LS, et al. A preoperative decolonization protocol for *Staphylococcus aureus* prevents orthopaedic infections. *Clin Orthopaed Relat Res.* 2008; 466:1343–1348.
5. Kluin OS, van der Mei HC, Busscher HJ, et al. Biodegradable vs non-biodegradable antibiotic delivery devices in the treatment of osteomyelitis. *Exp Opin Drug Deliv.* 2013; 10:341–351.
6. Zalavras CG, Patzakis MJ, Thordarson DB, et al. Infected fractures of the distal tibial metaphysis and plafond: achievement of limb salvage with free muscle flaps, bone grafting, and ankle fusion. *Clin Orthopaed Relat Res.* 2004; 427:57–62.
7. Beenken KE, Bradney L, Bellamy W, et al. Use of xylitol to enhance the therapeutic efficacy of polymethylmethacrylate-based antibiotic therapy in treatment of chronic osteomyelitis. *Antimicrob Agent Chemother.* 2012; 56:5839–5844.
8. Gitelis S, Brebach GT. The treatment of chronic osteomyelitis with a biodegradable antibiotic-impregnated implant. *J Orthopaed Surg.* 2002; 10:53–60.
9. Gogia JS, Meehan JP, Di Cesare PE, et al. Local antibiotic therapy in osteomyelitis. *Semin Plast Surg.* 2009; 23:100–107. [PubMed: 20567732]
10. Richelsoph KC, Webb ND, Haggard WO. Elution behavior of daptomycin-loaded calcium sulfate pellets: a preliminary study. *Clin Orthopaed Relat Res.* 2007; 461:68–73.
11. Thomas DB, Brooks DE, Bice TG, et al. Tobramycin-impregnated calcium sulfate prevents infection in contaminated wounds. *Clin Orthopaed Relat Res.* 2005; 441:366–371.
12. Turner TM, Urban RM, Hall DJ, et al. Local and systemic levels of tobramycin delivered from calcium sulfate bone graft substitute pellets. *Clin Orthopaed Relat Res.* 2005; 437:97–104.
13. von Stechow D, Scale D, Rauschmann MA. Minimizing the surgical approach in patients with spondylitis. *Clin Orthopaed Relat Res.* 2005; 439:61–67.
14. Jayakumar R, Ramachandran R, Sudheesh Kumar PT, et al. Fabrication of chitin-chitosan/nano ZrO₂ composite scaffolds for tissue engineering applications. *Int J Biol Macromol.* 2011; 49:274–280. [PubMed: 21575656]
15. De Castro GP, Dowling MB, Kilbourne M, et al. Determination of efficacy of novel modified chitosan sponge dressing in a lethal arterial injury model in swine. *J Trauma Acute Care Surg.* 2012; 72:899–907. [PubMed: 22491602]
16. Pusateri AE, McCarthy SJ, Gregory KW, et al. Effect of a chitosan-based hemostatic dressing on blood loss and survival in a model of severe venous hemorrhage and hepatic injury in swine. *J Trauma.* 2003; 54:177–182. [PubMed: 12544915]
17. Norowski PA, Courtney HS, Babu J, et al. Chitosan coatings deliver antimicrobials from titanium implants: a preliminary study. *Implant Dent.* 2011; 20:56–67. [PubMed: 21278528]
18. Smith JK, Bumgardner JD, Courtney HS, et al. Antibiotic-loaded chitosan film for infection prevention: a preliminary in vitro characterization. *J Biomed Mater Res, Part B: Appl Biomater.* 2010; 94:203–211. [PubMed: 20524196]
19. Fujimoto T, Tsuchiya Y, Terao M, et al. Antibacterial effects of chitosan solution against *Legionella pneumophila*, *Escherichia coli*, and *Staphylococcus aureus*. *Int J Food Microbiol.* 2006; 112:96–101. [PubMed: 17045689]
20. Jarmila V, Vavrikova E. Chitosan derivatives with antimicrobial, antitumour and antioxidant activities—a review. *Curr Pharm Des.* 2011; 17:3596–3607. [PubMed: 22074429]

21. Cho YW, Cho YN, Chung SH, et al. Water-soluble chitin as a wound healing accelerator. *Biomaterials*. 1999; 20:2139–2145. [PubMed: 10555081]
22. Patel MP, Patel RR, Patel JK. Chitosan mediated targeted drug delivery system: a review. *J Pharm Pharm Sci*. 2010; 13:536–557. [PubMed: 21486530]
23. Stinner DJ, Noel SP, Haggard WO, et al. Local antibiotic delivery using tailorable chitosan sponges: the future of infection control? *J Orthopaed Trauma*. 2010; 24:592–597.
24. Weiss BD, Weiss EC, Haggard WO, et al. Optimized elution of daptomycin from polymethylmethacrylate beads. *Antimicrob Agent Chemother*. 2009; 53:264–266.
25. Smeltzer MS, Thomas JR, Hickmon SG, et al. Characterization of a rabbit model of staphylococcal osteomyelitis. *J Orthopaed Res*. 1997; 15:414–421.
26. Kanellakopoulou K, Panagopoulos P, Giannitsioti E, et al. In vitro elution of daptomycin by a synthetic crystalline semihydrate form of calcium sulfate, stimulan. *Antimicrob Agent Chemother*. 2009; 53:3106–3107.
27. Webb ND, McCanless JD, Courtney HS, et al. Daptomycin eluted from calcium sulfate appears effective against *Staphylococcus*. *Clin Orthopaed Relat Res*. 2008; 466:1383–1387.
28. Zhang Y, Zhang M. Calcium phosphate/ chitosan composite scaffolds for controlled in vitro antibiotic drug release. *J Biomed Mater Res*. 2002; 62:378–386. [PubMed: 12209923]
29. Zhao J, Shen G, Liu C, et al. Enhanced healing of rat calvarial defects with sulfated chitosan-coated calcium deficient hydroxyapatite/bone morphogenetic protein 2 scaffolds. *Tissue Eng Part A*. 2012; 18:185–197. [PubMed: 21830854]
30. Cui X, Zhang B, Wang Y, et al. Effects of chitosan coated pressed calcium sulfate pellet combined with recombinant human bone morphogenetic protein 2 on restoration of segmental bone defect. *J Craniofac Surg*. 2008; 19:459–465. [PubMed: 18362727]
31. Reves BT, Bumgardner JD, Cole JA, et al. Lyophilization to improve drug delivery for chitosan-calcium phosphate bone scaffold construct: a preliminary investigation. *J Biomed Mater Res, Part B: Appl Biomater*. 2009; 90:1–10. [PubMed: 19441116]
32. Abarrategi A, Moreno-Vicente C, Ramos V, et al. Improvement of porous beta-TCP scaffolds with rhBMP-2 chitosan carrier film for bone tissue application. *Tissue Eng, Part A*. 2008; 14:1305–1319. [PubMed: 18491953]
33. Doty HA, Leedy MR, Courtney HS, et al. Composite chitosan and calcium sulfate scaffold for dual delivery of vancomycin and recombinant human bone morphogenetic protein-2. *J Mater Sci Mater Med*. Prepublished January 27, 2014. 10.1007/s10856-014-5167-7
34. Buranapanitkit B, Srinilta V, Ingvinga N, et al. The efficacy of a hydroxyapatite composite as a biodegradable antibiotic delivery system. *Clin Orthopaed Relat Res*. 2004; 424:244–252.
35. Buranapanitkit B, Oungbho K, Ingviya N. The efficacy of hydroxyapatite composite impregnated with amphotericin B. *Clin Orthopaed Relat Res*. 2005; 437:236–241.
36. Di Martino A, Sittinger M, Risbud MV. Chitosan: a versatile biopolymer for orthopaedic tissue-engineering. *Biomaterials*. 2005; 26:5983–5990. [PubMed: 15894370]
37. Parker AC, Jennings JA, Bumgardner JD, et al. Preliminary investigation of crosslinked chitosan sponges for tailorable drug delivery and infection control. *J Biomed Mater Res, Part B: Appl Biomater*. 2013; 101:110–123. [PubMed: 22997172]
38. Smith JK, Moshref AR, Jennings JA, et al. Chitosan sponges for local synergistic infection therapy: a pilot study. *Clin Orthopaed Relat Res*. 2013; 471:3158–3164.
39. Rouse MS, Piper KE, Jacobson M, et al. Daptomycin treatment of *Staphylococcus aureus* experimental chronic osteomyelitis. *J Antimicrob Chemother*. 2006; 57:301–305. [PubMed: 16361330]
40. Mader JT, Adams K. Comparative evaluation of daptomycin (LY146032) and vancomycin in the treatment of experimental methicillin-resistant *Staphylococcus aureus* osteomyelitis in rabbits. *Antimicrob Agent Chemother*. 1989; 33:689–692.
41. Poepl W, Tobudic S, Lingscheid T, et al. Daptomycin, fosfomicin, or both for treatment of methicillin-resistant *Staphylococcus aureus* osteomyelitis in an experimental rat model. *Antimicrob Agent Chemother*. 2011; 55:4999–5003.
42. Norden CW. Lessons learned from animal models of osteomyelitis. *Rev Infect Dis*. 1988; 10:103–110. [PubMed: 3281217]

43. Cremieux AC, Carbon C. Experimental models of bone and prosthetic joint infections. *Clin Infect Dis Off Publ Infect Dis Soc Am*. 1997; 25:1295–1302.
44. Yin LY, Lazzarini L, Li F, et al. Comparative evaluation of tigecycline and vancomycin, with and without rifampicin, in the treatment of methicillin-resistant *Staphylococcus aureus* experimental osteomyelitis in a rabbit model. *J Antimicrob Chemother*. 2005; 55:995–1002. [PubMed: 15857944]
45. Lazzarini L, Overgaard KA, Conti E, et al. Experimental osteomyelitis: what have we learned from animal studies about the systemic treatment of osteomyelitis? *J Chemother*. 2006; 18:451–460. [PubMed: 17127219]
46. Nelson CL, McLaren SG, Skinner RA, et al. The treatment of experimental osteomyelitis by surgical debridement and the implantation of calcium sulfate tobramycin pellets. *J Orthopaed Res Off Publ Orthopaed Res Soc*. 2002; 20:643–647.
47. Walsh WR, Morberg P, Yu Y, et al. Response of a calcium sulfate bone graft substitute in a confined cancellous defect. *Clin Orthopaed Relat Res*. 2003; 406:228–236.
48. Turner TM, Urban RM, Gitelis S, et al. Radiographic and histologic assessment of calcium sulfate in experimental animal models and clinical use as a resorbable bone-graft substitute, a bone-graft expander, and a method for local antibiotic delivery. One institution's experience. *J Bone Joint Surg Am Vol*. 2001; 83A(Suppl 2 Pt 1):8–18.
49. Gitelis S, Piasecki P, Turner T, et al. Use of a calcium sulfate-based bone graft substitute for benign bone lesions. *Orthopedics*. 2001; 24:162–166. [PubMed: 11284599]
50. Borrelli J Jr, Prickett WD, Ricci WM. Treatment of nonunions and osseous defects with bone graft and calcium sulfate. *Clin Orthopaed Relat Res*. 2003; 411:245–254.
51. Cho BC, Kim TG, Yang JD, et al. Effect of calcium sulfate-chitosan composite: pellet on bone formation in bone defect. *J Craniofac Surg*. 2005; 16:213–224. discussion 225–217. [PubMed: 15750417]
52. Chen H, Cui X, Yu X, et al. Effects of chitosan-coated pressed calcium sulfate pellets combined with recombinant human bone morphogenetic protein 2 on bone formation in femoral condyle-contained bone defects. *J Craniofac Surg*. 2010; 21:188–197. [PubMed: 20098183]
53. Muzzarelli RA, Mattioli-Belmonte M, Tietz C, et al. Stimulatory effect on bone formation exerted by a modified chitosan. *Biomaterials*. 1994; 15:1075–1081. [PubMed: 7888578]
54. Muzzarelli RAA. Chitosan composites with inorganics, morphogenetic proteins and stem cells, for bone regeneration. *Carbohydr Polym*. 2011; 83:1433–1445.
55. Hamilton V, Yuan YL, Rigney DA, et al. Bone cell attachment and growth on well-characterized chitosan films. *Polym Int*. 2007; 56:641–647.
56. Leedy MR, Martin HJ, Norowski PA, et al. Use of chitosan as a bioactive implant coating for bone-implant applications. *Chitosan Biomater II*. 2011; 244:129–165.
57. Bumgardner JD, Wisner R, Gerard PD, et al. Chitosan: potential use as a bioactive coating for orthopaedic and craniofacial/dental implants. *J Biomater Sci Polym Ed*. 2003; 14:423–438. [PubMed: 12807145]
58. Zugravu MV, Smith RA, Reves BT, et al. Physical properties and in vitro evaluation of collagen-chitosan-calcium phosphate microparticle-based scaffolds for bone tissue regeneration. *J Biomater Appl*. 2013; 28:566–579. [PubMed: 23128039]
59. Chesnutt BM, Yuan Y, Brahmandam N, et al. Characterization of biomimetic calcium phosphate on phosphorylated chitosan films. *J Biomed Mater Res Part A*. 2007; 82:343–353.
60. Elder S, Gottipati A, Zelenka H, et al. Attachment, proliferation, and chondroinduction of mesenchymal stem cells on porous chitosan-calcium phosphate scaffolds. *Open Orthopaed J*. 2013; 7:275–281.
61. Wang J, de Boer J, de Groot K. Proliferation and differentiation of MC3T3-E1 cells on calcium phosphate/chitosan coatings. *J Dent Res*. 2008; 87:650–654. [PubMed: 18573985]
62. Cho BC, Chung HY, Lee DG, et al. The effect of chitosan bead encapsulating calcium sulfate as an injectable bone substitute on consolidation in the mandibular distraction osteogenesis of a dog model. *J Oral Maxillofac Surg: Off J Am Assoc Oral Maxillofac Surg*. 2005; 63:1753–1764.
63. Rabea EI, Badawy ME, Stevens CV, et al. Chitosan as antimicrobial agent: applications and mode of action. *Biomacromolecules*. 2003; 4:1457–1465. [PubMed: 14606868]

64. Ong SY, Wu J, Moochhala SM, et al. Development of a chitosan-based wound dressing with improved hemostatic and antimicrobial properties. *Biomaterials*. 2008; 29:4323–4332. [PubMed: 18708251]
65. Raafat D, Sahl HG. Chitosan and its antimicrobial potential—a critical literature survey. *Microbiol Biotechnol*. 2009; 2:186–201.
66. Dai T, Tanaka M, Huang YY, et al. Chitosan preparations for wounds and burns: antimicrobial and wound-healing effects. *Expert Rev Anti-infect Ther*. 2011; 9:857–879. [PubMed: 21810057]
67. Simunek J, Brandysova V, Koppova I, et al. The antimicrobial action of chitosan, low molar mass chitosan, and chitooligosaccharides on human colonic bacteria. *Folia Microbiol*. 2012; 57:341–345. [PubMed: 22528310]
68. Kim KW, Thomas RL, Lee C, et al. Antimicrobial activity of native chitosan, degraded chitosan, and *O*-carboxymethylated chitosan. *J Food Protect*. 2003; 66:1495–1498.

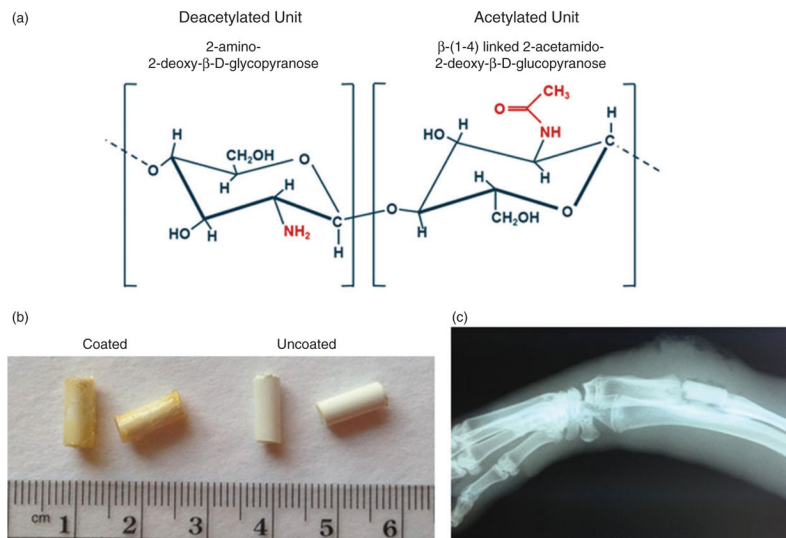


Figure 1. Chitosan coating of calcium sulfate pellets. (a) Structural characteristics of deacetylated versus acetylated chitosan units. (b) Comparison of coated versus uncoated calcium sulfate pellets. (c) Representative radiograph of antibiotic-loaded chitosan coated implant (15 C) immediately post debridement and implantation.

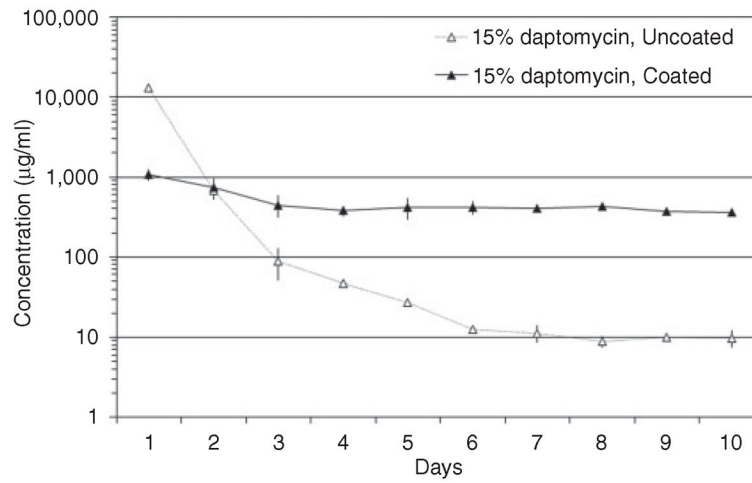


Figure 2. Elution profile as a function of chitosan coating. Daptomycin concentrations were determined using high-pressure liquid chromatography at daily intervals after complete replacement of the elution buffer. The breakpoint MIC for a daptomycin-sensitive strain of *S. aureus* is 1.0 µg/ml.

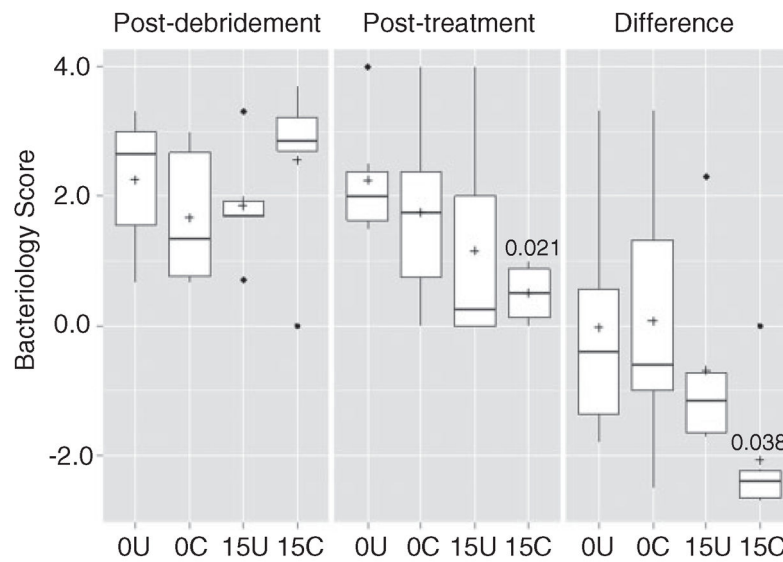


Figure 3. Analysis based on average bacteriological scores. Results are shown for each experimental group immediately following debridement, after treatment, and as the change between these two time points. 0U and 0C refer to uncoated and coated pellets, respectively, while 15U and 15C refer to uncoated and coated pellets containing daptomycin. Boxes indicate the 25th and 75th percentiles for each group and define the IQR, with the horizontal line indicating the median. Vertical lines define the lowest and highest data points within 1.5 IQR of the lower and higher quartiles, respectively, with individual dots representing single data points outside this range. Numbers within the graph are p values determined as described in the text. IQR: interquartile range.

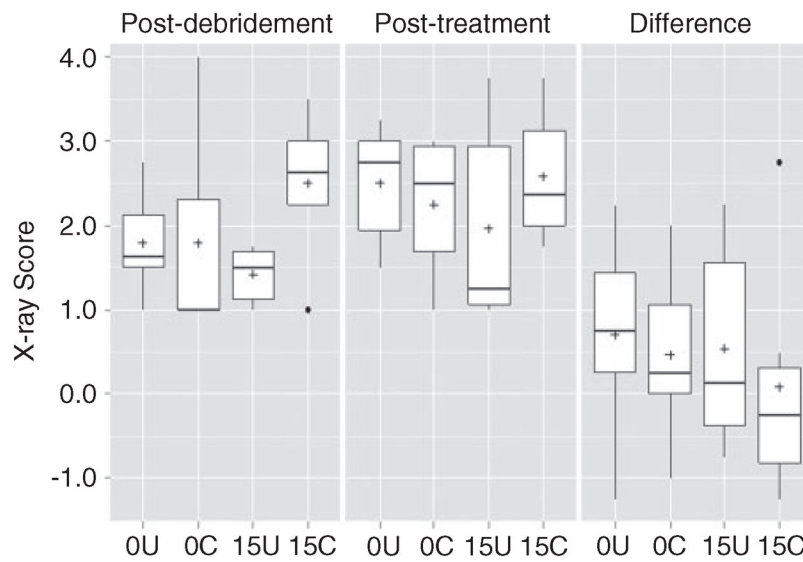


Figure 4. Analysis based on average X-ray scores. Results are shown for each experimental group immediately following debridement, after treatment, and as the change between these two time points. 0U and 0C refer to uncoated and coated pellets, respectively, while 15U and 15C refer to uncoated and coated pellets containing daptomycin. None of the differences observed by X-ray were statistically significant. Boxes indicate the 25th and 75th percentiles for each group and define the IQR, with the horizontal line indicating the median. Vertical lines define the lowest and highest data points within 1.5 IQR of the lower and higher quartile, respectively, with individual dots representing single data points outside this range. Numbers within the graph are p values determined as described in the text.

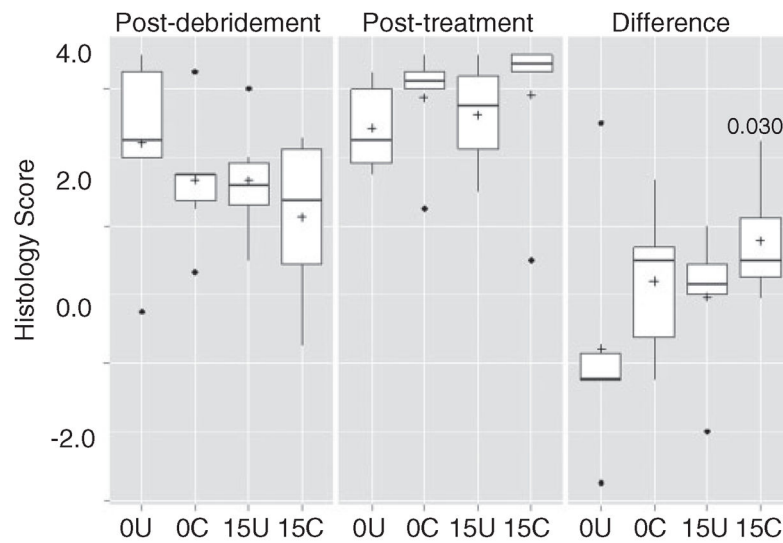


Figure 5. Analysis based on average histopathological scores. Results are shown for each experimental group immediately following debridement, after treatment, and as the change between these two time points. 0U and 0C refer to uncoated and coated pellets, respectively, while 15U and 15C refer to uncoated and coated pellets containing daptomycin. Boxes indicate the 25th and 75th percentiles for each group and define the IQR, with the horizontal line indicating the median. Vertical lines define the lowest and highest data points within 1.5 IQR of the lower and higher quartiles, respectively, with individual dots representing single data points outside this range. Numbers within the graph are p values determined as described in the text.

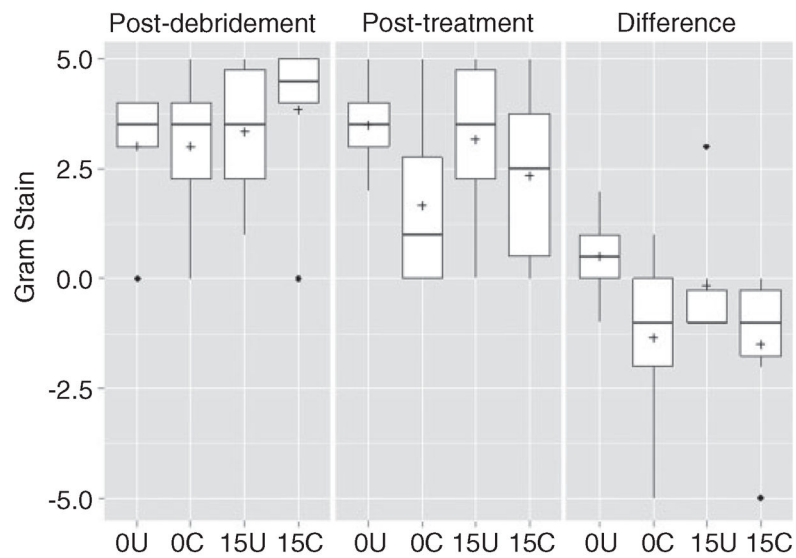


Figure 6. Analysis based on average Gram stain scores. Results are shown for each experimental group immediately following debridement, after treatment, and as the change between these two time points. None of the differences observed by Gram stain were statistically significant. 0U and 0C refer to uncoated and coated pellets, respectively, while 15U and 15C refer to uncoated and coated pellets containing daptomycin. Boxes indicate the 25th and 75th percentiles for each group and define the IQR, with the horizontal line indicating the median. Vertical lines define the lowest and highest data points within 1.5 IQR of the lower and higher quartiles, respectively, with individual dots representing single data points outside this range. Numbers within the graph are p values determined as described in the text.

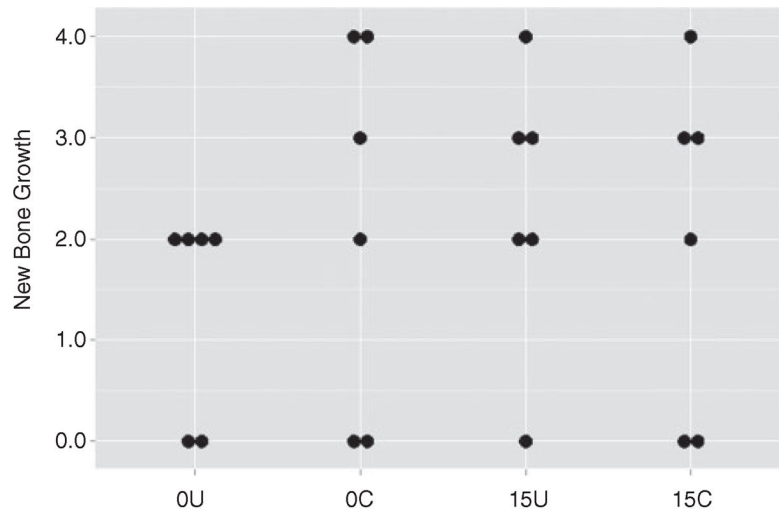


Figure 7. Assessment of new bone growth. Results are shown for individual mice within each experimental group following treatment based on histopathological analysis. 0U and 0C refer to uncoated and coated pellets, respectively, while 15U and 15C refer to uncoated and coated pellets containing daptomycin. None of the differences between groups were statistically significant.